

In-Silico analysis and molecular docking studies of phytoconstituents of *Justicia adhatoda* as potential inhibitors of SARS-CoV2 target proteins

Abhinayaa Ananth Suryanarayana, Soundarya Shankar, Jeevitha Priya Manoharan,
Subramanian Vidyalakshmi *

{ abhinayaananth@gmail.com, soundaryashankar2000@gmail.com, jeevithapriya2005@gmail.com,
svd.bio@psgtech.ac.in }

Department of Biotechnology, PSG College of Technology, Coimbatore, Tamil Nadu, India.

Abstract. The outbreak of COVID 19, a pandemic disease spread by the novel Coronavirus-SARS- CoV-2 infection, there is an emerging necessity to identify potential and effective therapeutic drug candidates. Many researchers have focused on exploiting the antiviral properties of phytochemicals from traditionally used medicinal plants. Computational prediction of drug candidates has shown prospects in the identification of therapeutic targets of SARS-CoV-2. Our current study explores the possibility of identifying potential anti-COVID candidates from the phytochemicals of *Justicia adhatoda* by virtual screening. Molecular docking analysis of these lead compounds were performed at the binding pockets of 10 viral proteins. The compounds were analyzed for their ADMET properties, drug-likeness, and bioactivity to examine their druggability. Our findings indicate that 51.5% of phytochemicals from *Justicia adhatoda* are druggable against COVID-19. It was also found that the phytochemicals xanthoxylol, podophyllotoxin, quercetin, chinensinaphthol methyl ether, and apigenin could act as potential lead molecules against multiple target proteins of SARS- CoV-2..

Keywords: SARS-CoV 2, *Justicia adhatoda*, Phytochemicals, Molecular docking, ADMET, Anti-COVID drug.

1 Introduction

Severe Acute Respiratory Syndrome – Coronavirus - 2 (SARS-CoV-2), which has led to the ongoing Covid-19 pandemic, has posed a serious health threat across the entire globe. The World Health Organization (WHO) has announced 24,257,989 confirmed cases of COVID-19, leading to 827,246 deaths across the globe as on 10 July 2020 (<https://covid19.who.int/>). Currently, there are no effective drugs or vaccines available to protect us from the virus. Several medicinal plants have been reported to possess anti viral effects on herpes simplex virus type 2 (HSV-2) (Debiaggi et al., 1988), HIV (Asres and Bucar, 2005) and emerging severe acute respiratory syndrome (SARS) virus (Kotwal et al., 2005). Naturally occurring phytochemicals have also been shown to exhibit several pharmacological properties like immunostimulatory properties (Webster et al., 2006), inhibitory effects on viral protease (Mukhtar et al, 2008), and anti-inflammatory properties (Hajjaj et al., 2013). Bioactive compounds from medicinal plants are particularly advantageous due to their ease of

availability and lesser side effects. Phytocompounds are also preferred than synthetic compounds as repurposing these compounds from plants is less time consuming than developing a new molecule from the scratch. The plant chosen in this work is *Justicia adhatoda*, which is traditionally used as an expectorant for treating respiratory disorders (Murugesu mudhaliar KS., 2006). Studies have also shown that the extracts of this plant inhibited influenza virus attachment and/or viral replication (Shahid et al., 2013).

Drug discovery is a very challenging process. Of late, exploiting computational tools for novel drug development had shortened the time taken for the drug discovery process and also made the process very efficient. Molecular docking, molecular simulation, and virtual screening are valuable tools for screening potential drugs/molecules from various databases that have enormous data on various compounds (Wadood et al., 2013). One of the crucial steps in in silico drug designing is selecting the drug targets from the pathogen (Eweas et al., 2014). The number of SARS-CoV-2 structures deposited in the RCSB Protein Data Bank is tremendously increasing (RCSB PDB). An extensive literature survey showed that the proteins involved in viral entry (Spike glycoprotein) (Prasanth et al., 2020; Hall and Ji, 2020; UNNI et al., 2020) and replication (16 non-structural proteins) (Islam et al., 2020; Sinha et al., 2020; Chikhale et al., 2020; Azim et al., 2020) can be targeted for drug discovery.

Coronavirus has been reported to possess at least six ORFs in its genome. Around 16 NSPs (nsp1-16) constitute about two-thirds of the entire genome length. ORF1a and ORF1b are cleaved to form the two polypeptides: pp1a and pp1ab, which are processed by chymotrypsin-like protease (3CLpro) or main protease (Mpro) and one or two papain-like proteases to generate 16 NSPs. These proteins are generated from the single guide RNAs of CoVs. The structural proteins spike (S), membrane (M), envelope (E), and nucleocapsid (N) proteins are encoded by ORFs 10, 11 (Shaikh et al., 2007). The virus also encode special proteins, including hemagglutinin esterase protein, 3a/b protein, and 4a/b protein. These proteins are necessary for genome maintenance and virus replication. The spike (S) protein is responsible for the viral entry into target cells, which is dependent on the binding of its surface unit, S1 to a cellular receptor. This further facilitates viral attachment to the target cells. (Hoffmann et al., 2013). NSP 3 and nsp4 are involved in the assembly of virally induced vesicles necessary for viral replication. Nsp3 releases Nsp1, Nsp2, and interacts with other NSPs and RNA to form the replication/transcription complex. Nsp3 also antagonize the host innate immune response. Nsp3 also interact with host proteins (such as RCHY1) to support viral survival (Lei et al., 2018). Nsp9 is involved in the transcription and replication of viral RNAs (Sutton et al., 2004). SARS-CoV has been shown to interact with angiotensin-converting enzyme 2 (ACE2) to initiate its entry into the target cells (Li, 2008; Kirchdoerfer et al., 2018; Li et al., 2003).

It was shown by Liu wenzhong and Li hualan (2020) that ORF1ab, ORF10, and ORF3a proteins attack heme and dissociate iron to generate porphyrin. This is responsible for the respiratory failure in the host system. Lack of oxygen causes leads to multiple organ failure (Abhrajit and Arijit, 2020). These studies were carefully investigated for choosing the drug targets of SARS-CoV2. Hence, in this analysis, 10 structural and non-structural proteins of SARS-CoV2 were used for identifying potential lead compounds against them.

Our current study aims in identifying an effective lead molecule against the virus from natural sources. Kabasura kudineer, a Siddha formulation used against fevers leading to respiratory infections showed activity against viral proteins and also modulates the host immune system. Most of the phytocompounds prevented the binding of viral protein with the receptor (Pitchiah Kumar et al., 2020).

Justicia adhatoda, one of the plants which comprise a major part in the Kabasura kudineer formulation was chosen for screening potential inhibitors against ten of the SARS-CoV-2 proteins. Previous studies support the usage of the extract of *Justicia adhatoda* as a remedy for the patients affected by COVID-19 (Abhrajit and Arijit, 2020; Corrêa et al., 2012). Virtual docking analysis was performed against the target proteins to identify potential lead molecules which might act as inhibitors of COVID-19.

2 Materials And Methods

Selection of Ligands:

An exhaustive review of scientific literature was done to screen for the various phytochemicals present in *Justicia adhatoda* (Thokchom et al., 2011). An extensive library of phytochemicals having 87 active compounds (**Supplementary Table 1**) was pooled and the library was constructed with 68 molecules. The 3D structure of the 68 phytochemicals (**Supplementary Table 2**) was retrieved from the PubChem database (<https://pubchem.ncbi.nlm.nih.gov/>) in SDF format. Compounds lacking structures in any of the databases and literature were neglected for the current study.

Drug likeness properties:

Drug likeness properties of the phytochemicals were computed using SWISS ADME (Daina et al., 2017), an online tool based on Lipinski's rule of five (Ro5). The rule was developed to set drug ability guidelines for new molecular entities and predicts that molecules are more likely to show good absorption when there are less than 5 H-bond donors and 10 H-bond acceptors, for ligands with a molecular weight lesser than 500 Da and whose calculated Log P is less than 5 (Lipinski et al., 2001). Ligands obeying the rule of five were taken for ligand preparation for performing molecular docking studies.

Ligand preparation:

The ligands were prepared to ensure that the atoms in the ligand molecules are assigned to the correct Autodock 4 atom types required to run Autodock VINA simulation. Autodock 4 (AD4) atom types are similar to that of the elements in most atoms except for the replacement of hydrogen-bond acceptors O, N and S atoms with "OA", "NA" and "SA"; hydrogen-bond donor H atoms with "HD"; non-hydrogen bonding nitrogen with "N" and "A" for carbons in aromatic rings. PDBQT format is identical to PDB format but includes partial charges (Q) and AD4 atom types (T). 35 Ligands obeying the Lipinski rule of five along with 10 FDA approved repurposed COVID 19 drugs (Positive controls) were included for the study and are listed along with their chemical structures in **Table 1**. The ligands were prepared in AUTODOCK tools by the addition of Gasteiger charges for docking analysis. Further non-polar hydrogen bonds were merged for the ligands and the file was stored in PDBQT format.

Protein preparation:

The X-ray diffraction-based 3D crystal structures of 10 essential SARS-CoV-2 proteins were downloaded in PDB format from the RCSB PDB (<https://www.rcsb.org/>) database. An open-source molecular visualization tool: The PyMOL Molecular Graphics System, Version 1.2r3pre, Schrödinger, LLC. was used to clean the proteins by removing the water molecules, ions, and ligands present in the retrieved proteins. All the proteins were energy minimized using the Swiss- PDB Viewer. The Graphical user interface software AUTODOCK tools was used to prepare the protein by deleting het group water molecules. Addition of Kollman

charges and polar hydrogen bonds were performed and the prepared proteins were stored in PDBQT format for docking analysis.

Active site prediction of the proteins and grid generation:

Active site residues of the target proteins were predicted using METAPOCKET 2.0, an online meta server which is a combination of the following eight methods: LIGSITEcs, PASS, Q-SiteFinder, SURFNET, Fpocket, GHECOM, ConCavity and POCASA for better prediction rates (Huang, 2009). Docking simulations in Autodock Vina 1.1.2 were done by the generation of specific grids around the active site residues reported at the top hit of each protein. The parameters used for grid generation are listed in **Table 2**.

Molecular docking:

Molecular docking is employed to identify the essential amino acid interactions between the selected protein and generated ligands with low energy conformation (Carlesso et al., 2019). Autodock Vina 1.1.2 (Trott and Olson, 2010) was used to perform 10 runs of flexible docking for each protein with the phytocompounds and 10 repurposed COVID drugs individually using AutoDockZN forcefield with the recognized active site placed within the constructed grid. Docking scores were reported in kcal/mol and compounds with a threshold value lesser than -7 kcal/mol were analyzed further for protein-ligand interaction. Identification of ligand interactions in the protein-ligand complexes reports the critical residues involved in the interaction and nature of their interaction. This study is performed using Protein- Ligand Interaction Profiler (PLIP) (Salentin et al., 2015). Two-dimensional LIGPLOT (Wallace et al., 1995) representations of receptor-ligand interaction were generated with PDBsum: a pictorial database (<http://www.ebi.ac.uk/pdbsum>).

ADMET analysis of Phytocompounds:

ADMET analysis was performed for the top scoring ligands (**Supplementary Table 3**) which reported several pharmacokinetic properties including water solubility, intestinal absorption, CYP inhibition, blood brain barrier permeability, total clearance, maximum recommended tolerated dose and acute rat toxicity dosage. Toxicity profiles of individual phytocompounds were also generated with the pkCSM Biosig online server (Pires et al., 2015). AMES toxicity is predicted to determine if the compound could be mutagenic. On the other hand, hepatotoxicity plays an important safety concern in drug development which may lead to drug attrition and may disrupt the normal function of the liver. Thus, phytocompounds which were negative for both AMES and hepatotoxicity tests were taken forward for ligand interaction studies as these molecules will show no indication of carcinogenicity as well as chemical driven liver damage.

PASS computer program

Prediction of Activity Spectra for Substances (PASS) was determined using the PASS Online tool, a computer-based program providing biological activity, to check the ability of phytocompounds to interact with various biological molecules by predicting probable activity (Pa) and probable inactivity (Pi). The substances possessing a higher Pa than Pi are favorable drug molecules (Goel et al., 2011; Khurana et al., 2011). The antiviral activity was predicted for the lead compounds.

3 Results And Discussion

Studies suggest that natural compounds can be used to target several human diseases (Pop et al., 2018). In this context, medicinal plants display themselves as valuable sources of drugs to treat many ailments and infectious diseases. Also, Indian medicinal plants have been used by the traditional Ayurveda, Siddha, and Unani based systems of medicine since several years (<https://www.nmpb.nic.in/content/medicinal-plants-fact-sheet>). There has been an enormous interest in the screening of phytochemicals as drug source. Plants have been the primary sources of medicine for early drug discovery (Veeresham, 2012). Our current study looks out for anti-COVID compounds from the plant *Justicia adhatoda* through computational molecular docking and drug prediction studies.

Analysis of drug-likeness properties

A wide range of phytochemicals of *J. adhatoda* possessing various pharmacological activities such as antimicrobial (Sarker et al., 2009), bronchodilator activity (Dorsch and Wagner, 1991), anti-allergic (Paliwa et al., 2000), anti-asthmatic (Wagner, 1989), anti-inflammatory (Chakraborty and Brantner, 2001) and abortifacient (Claeson et al., 2000) have been picked up from literature analysis and a schematic representation of initial screening of compounds is depicted in **Figure 1**. Drug likeness properties of 68 compounds were assessed by an online server SWISS ADME. 35 phytochemicals were found to obey the Lipinski rule of five criteria. The molecular weight of the selected compounds was within the range of 162 – 414 Da. About 26% of the screened compounds were found to possess 6 hydrogen bond acceptors. Similarly, 40% of the filtered compounds were noticed to have zero hydrogen bond donors. A Log P value of the compounds was within the range of 0.4 – 3.7, indicating that the compounds were lipophilic in nature. These results show that the phytochemicals selected for our study are likely having good absorption and permeation properties in the biological system and might act as potential drug candidates. Lipinski's rule of five parameters of phytochemicals are listed in **Table 3**.

Toxicity profiles

The toxicity profiles of the phytochemicals were predicted and summarized in **Table 4**. The toxicity profile includes ten parameters namely AMES toxicity, maximum tolerated human dose, herG I inhibitor, herG II inhibitor, oral rat acute toxicity, oral rat chronic toxicity, hepatotoxicity, skin sensitization, T. pyriformis toxicity, and minnow toxicity. The analysis predicted that 12 of these phytochemicals (**Figure 2**) were nontoxic and could be potential drug candidates.

Molecular Docking studies

The 12 nontoxic phytochemicals and 10 FDA approved COVID-19 repurposed drugs were screened against 10 target proteins of coronavirus using Autodock VINA 1.1.2. The docking score of the phytochemicals is represented in kcal/mol and summarized in **Table 5**. The docking scores of FDA approved drugs is given in **Table 6**. The majority of the phytochemicals showed good docking affinity with the target proteins in the range of -5.9 to -9.5 kcal/mol. The affinity of the repurposed drugs is in the range of -4.6 to -10.4 kcal/mol. **Figure 3** represents the percentage of phytochemicals with a favorable binding affinity against the target proteins of COVID-19. Nearly 88.57 percentage of the compounds showed a higher binding affinity to the spike protein of coronavirus and therefore these compounds might act as a barrier for attachment of the viral protein with the host cell. From our analysis, it was seen that the most potent inhibitor for the main protease is chinensinaphthol methyl ether (-8 kcal/mol). This compound also showed the highest binding affinity of -8.8 kcal/mol for the spike protein – RBD complex. Luteolin binds with the highest affinity to spike protein

(-9.1 kcal/mol). Among the repurposed drugs, darunavir was found to possess the most favourable docking scores against multiple proteins like envelope protein (-10.6 kcal/mol), spike protein (-10.3 kcal/mol) and membrane protein (-10.2 kcal/mol). It was also observed that a majority of the ligands showed favourable docking interaction with all the target proteins.

A heatmap represented in **Figure 4** was generated to indicate the degree of relatedness of the target proteins and the ligands. It can be seen that the target protein bifurcates into two classes. Spike protein, spike protein – RBD complex, and nsp9 are closer in the tree and the other proteins are clustered as a separate class. This indicates that most of the ligands had a similar binding affinity for these proteins. Similarly, the clustering pattern of the ligands is also shown in the generated heat map. It can be observed that the repurposed drug darunavir, which showed the maximum binding affinity with many target proteins, is distantly related to the phytochemicals indicating a different mechanism of action.

Two-dimensional ligand interaction profile

To evaluate the binding interaction of the docked protein-ligand complexes, 2D protein-ligand interaction profiling was done for both phytochemicals and FDA approved repurposed drugs (**Supplementary Table 4**) and the residues involved in hydrogen bond formation and hydrophobic interactions are summarized and represented in **Table 7,8** and **Figure 5**. Hydrogen bonds are of great importance in protein folding, protein ligand interaction, and catalysis. Quercetin showed the highest number of hydrogen bonds formed with the Spike protein among all the top-scoring ligands with an affinity of -9.1 kcal/mol. Xanthoxylol on the other hand forms the highest number of hydrophobic interactions with the envelope protein with a docking affinity of -8.4 kcal/mol which is essential in increasing the binding affinity between the protein and ligand. As the number of hydrophobic atoms in the active core of the drug-target interface increases the biological activity of the drug also increases, making both xanthoxylol and quercetin highly versatile drug compounds capable of inhibiting most of the target proteins with great affinity. Ligand interactions were also studied for FDA approved repurposed COVID 19 drugs and it was noticed that similar patterns of interactions were observed for xanthoxylol and darunavir forming a hydrogen bond with the residue 26B TYR and hydrophobic interactions with the residues 63B TYR and 235A PRO of membrane protein. Similarly, chinensinaphthol methyl ether and hydroxychloroquine recognized alike interacting residues showing hydrogen bonds with 26A THR, 143A GLY and hydrophobic interactions with 165A MET in the main protease of coronavirus. These results suggest that few of our selected compounds such as chinensinaphthol methyl ether and xanthoxylol were showing greater accordance with the pattern of interactions of currently approved COVID drugs. Therefore, these phytochemicals can be utilized for inhibiting the target proteins of COVID-19 upon experimental validation.

4 ADMET analysis of lead molecules

ADMET prediction has a central role in determining the pharmacokinetic properties which is cardinal in any drug development and improve efficiency in eliminating weak candidates in the early stages. *In silico* methods were employed to predict absorption, distribution, metabolism, excretion, and toxicity of the 12 potential lead molecules passing the AMES and hepatotoxicity tests using the pkCSM approach. The ADME/T profiles of 12 phytochemicals are listed in **Table 9**. In comparison with the repurposed drugs, the ADMET

properties of the proposed ligands are at par. The ADMET properties of drug-like molecules demonstrated that the compounds possessed good water solubility and intestinal absorption. The lead molecules chinensinaphthol methyl ether, podophyllotoxin, quercetin, xanthoxylol showed intestinal absorption of 100%, 100%, 77.207%, 94.756% respectively. Other parameters exhibited satisfactory results as well. Many drugs are deactivated by cytochrome P450 and some are activated by it. Among the 12 lead-like compounds, chinensinaphthol methyl ether, heliobupthalmin, justiciresinol, podophyllotoxin, vasicilonone and xanthoxylol has the ability to act as CYP450 substrate. Considering the total clearance of these molecules, chinensinaphthol methyl ether has the highest clearance rate of about 0.461log ml/min/kg, the rest of them having acceptable clearance values. The intestinal absorption of lead molecules was more than 30% indicating that it can be highly absorbed and hence well suited for oral administration. From the other ADMET properties listed, it is suggested that the lead molecules are acceptable for human consumption although *in-vivo* validation is essential.

PASS profile

The antiviral activity of the lead molecules is assessed by PASS online tool and is summarized in **Table 10**. The predicted Pa and Pi values show that all lead compounds possessed a higher probability to be active against most viruses. Lead molecules, namely kaempferol, xanthoxylol, and quercetin were predicted to possess efficient antiviral activity. These results suggest that the lead molecules can be efficient in fighting against SARS CoV-2 also.

6 Conclusion

Considering this global threat of COVID-19 with no proven antiviral agents available for immediate recovery, our findings help in establishing a broader perspective of potential antiviral lead compounds from *Justicia adhatoda*. Most of the top-scoring ligands possessed remarkable ADME properties, but on narrowing down the ligands based on toxicity and other pharmacological properties, the phytocompounds xanthoxylol, apigenin, chinensinaphthol methyl ether, quercetin, and podophyllotoxin may serve as effective lead candidates to inhibit SARS-CoV2. Further experimental studies should be carried out for identified lead molecules for exploring the mechanism of inhibition against COVID-19.

Disclosure Statement

There is no potential conflict of interest.

Funding

There is no funding associated with this work.

References

- [1] Asres, K., & Bucar, F. (2005). Anti-HIV activity against immunodeficiency virus type 1 (HIV-I) and type II (HIV-II) of compounds isolated from the stem bark of *Combretum molle*. *Ethiopian medical journal*, 43(1), 15–20.
- [2] Azim, K. F., Ahmed, S. R., Banik, A., Khan, M., Deb, A., & Somana, S. R. (2020). Screening and druggability analysis of some plant metabolites against SARS-CoV-2: An integrative computational approach. *Informatics in medicine unlocked*, 20, 100367. <https://doi.org/10.1016/j.imu.2020.100367>
- [3] Bag, A., & Bag, A.. (2020). Treatment of COVID-19 patients: *Justicia adhatoda* leaves extract is a strong remedy for COVID-19 – Case report analysis and docking based study (Version 1). *ChemRxiv*. <https://doi.org/10.26434/chemrxiv.12038604.v1>
- [4] Carlesso, A., Chinthia, C., Gorman, A. M., Samali, A., & Eriksson, L. A. (2019). Merits and pitfalls of conventional and covalent docking in identifying new hydroxyl aryl aldehyde like compounds as human IRE1 inhibitors. *Scientific reports*, 9(1), 3407. <https://doi.org/10.1038/s41598-019-39939-z>
- [5] Chakraborty, A., & Brantner, A. H. (2001). Study of alkaloids from *Adhatoda vasica* Nees on their antiinflammatory activity. *Phytotherapy research : PTR*, 15(6), 532–534. <https://doi.org/10.1002/ptr.737>
- [6] Chikhale, R. V., Gurav, S. S., Patil, R. B., Sinha, S. K., Prasad, S. K., Shakya, A., Shrivastava, S. K., Gurav, N. S., & Prasad, R. S. (2020). Sars-cov-2 host entry and replication inhibitors from Indian ginseng: an in-silico approach. *Journal of biomolecular structure & dynamics*, 1–12. Advance online publication. <https://doi.org/10.1080/07391102.2020.1778539>
- [7] Claeson, U. P., Malmfors, T., Wikman, G., & Bruhn, J. G. (2000). *Adhatoda vasica*: a critical review of ethnopharmacological and toxicological data. *Journal of ethnopharmacology*, 72(1-2), 1–20. [https://doi.org/10.1016/s0378-8741\(00\)00225-7](https://doi.org/10.1016/s0378-8741(00)00225-7)
- [8] Corrêa, Geone M., & Alcântara, Antônio F. de C.. (2012). Chemical constituents and biological activities of species of *Justicia*: a review. *Revista Brasileira de Farmacognosia*, 22(1), 220-238. Epub November 01, 2011. <https://doi.org/10.1590/S0102-695X2011005000196>
- [9] Daina, A., Michielin, O. & Zoete, V. SwissADME: a free web tool to evaluate pharmacokinetics, drug-likeness and medicinal chemistry friendliness of small molecules. *Sci Rep* 7, 42717 (2017). <https://doi.org/10.1038/srep42717>
- [10] Debiaggi, M., Pagani, L., Cereda, P. M., Landini, P., & Romero, E. (1988). Antiviral activity of *Chamaecyparis lawsoniana* extract: study with herpes simplex virus type 2. *Microbiologica*, 11(1), 55–61.
- [11] Dorsch, W., & Wagner, H. (1991). New antiasthmatic drugs from traditional medicine?. *International archives of allergy and applied immunology*, 94(1-4), 262–265. <https://doi.org/10.1159/000235378>
- [12] Eweas, A.F., Maghrabi, I., & Namarneh, A.I. (2014). Advances in molecular modeling and docking as a tool for modern drug discovery. *Sch Res Lib Der Pharma Chem* 2014; 6:211e28.
- [13] Goel, R.K., Singh, D., Lagunin, A. et al. PASS-assisted exploration of new therapeutic potential of natural products. *Med Chem Res* 20, 1509–1514 (2011). <https://doi.org/10.1007/s00044-010-9398-y>
- [14] Hajjaj, G., Bounihi, A., Tajani, M., Cherrah, Y., Zellou, A., 2013a. Anti-inflammatory evaluation of aqueous extract of *Matricaria chamomilla* L. (asteraceae) in experimental animal models from Morocco. *World J. Pharm. Res.* 2 (5), 1218–1228.
- [15] Hall, D. C., Jr, & Ji, H. F. (2020). A search for medications to treat COVID-19 via in silico molecular docking models of the SARS-CoV-2 spike glycoprotein and 3CL protease. *Travel medicine and infectious disease*, 35, 101646. <https://doi.org/10.1016/j.tmaid.2020.101646>
- [16] Hoffmann, M., Müller, M. A., Drexler, J. F., Glende, J., Erdt, M., Gützkow, T., Losemann, C., Binger, T., Deng, H., Schwegmann-Weßels, C., Esser, K. H., Drosten, C., & Herrler, G. (2013). Differential sensitivity of bat cells to infection by enveloped RNA viruses: coronaviruses, paramyxoviruses, filoviruses, and influenza viruses. *PloS one*, 8(8), e72942. <https://doi.org/10.1371/journal.pone.0072942>
- [17] Huang B. (2009). MetaPocket: a meta approach to improve protein ligand binding site prediction. *Omics : a journal of integrative biology*, 13(4), 325–330. <https://doi.org/10.1089/omi.2009.0045>

- [18] Islam, R., Parves, M. R., Paul, A. S., Uddin, N., Rahman, M. S., Mamun, A. A., Hossain, M. N., Ali, M. A., & Halim, M. A. (2020). A molecular modeling approach to identify effective antiviral phytochemicals against the main protease of SARS-CoV-2. *Journal of biomolecular structure & dynamics*, 1–12. Advance online publication. <https://doi.org/10.1080/07391102.2020.1761883>
- [19] Khurana, N., Ishar, M. P., Gajbhiye, A., & Goel, R. K. (2011). PASS assisted prediction and pharmacological evaluation of novel nicotinic analogs for nootropic activity in mice. *European journal of pharmacology*, 662(1-3), 22–30. <https://doi.org/10.1016/j.ejphar.2011.04.048>
- [20] Kirchdoerfer, R. N., Wang, N., Pallesen, J., Wrapp, D., Turner, H. L., Cottrell, C. A., Corbett, K. S., Graham, B. S., McLellan, J. S., & Ward, A. B. (2018). Stabilized coronavirus spikes are resistant to conformational changes induced by receptor recognition or proteolysis. *Scientific reports*, 8(1), 15701. <https://doi.org/10.1038/s41598-018-34171-7>
- [21] Kotwal, G. J., Kaczmarek, J. N., Leivers, S., Ghebremariam, Y. T., Kulkarni, A. P., Bauer, G., De Beer, C., Preiser, W., & Mohamed, A. R. (2005). Anti-HIV, anti-poxvirus, and anti-SARS activity of a nontoxic, acidic plant extract from the *Trifolium* species Secomet-V/anti-vac suggests that it contains a novel broad-spectrum antiviral. *Annals of the New York Academy of Sciences*, 1056(1), 293–302. <https://doi.org/10.1196/annals.1352.014>
- [22] Lei, J., Kusov, Y., & Hilgenfeld, R. (2018). Nsp3 of coronaviruses: Structures and functions of a large multi-domain protein. *Antiviral research*, 149, 58–74. <https://doi.org/10.1016/j.antiviral.2017.11.001>
- [23] Li F. (2008). Structural analysis of major species barriers between humans and palm civets for severe acute respiratory syndrome coronavirus infections. *Journal of virology*, 82(14), 6984–6991. <https://doi.org/10.1128/JVI.00442-08>
- [24] Li, W., Moore, M. J., Vasileva, N., Sui, J., Wong, S. K., Berne, M. A., Somasundaran, M., Sullivan, J. L., Luzuriaga, K., Greenough, T. C., Choe, H., & Farzan, M. (2003). Angiotensin-converting enzyme 2 is a functional receptor for the SARS coronavirus. *Nature*, 426(6965), 450–454. <https://doi.org/10.1038/nature02145>
- [25] Lipinski, C. A., Lombardo, F., Dominy, B. W., & Feeney, P. J. (2001). Experimental and computational approaches to estimate solubility and permeability in drug discovery and development settings. *Advanced drug delivery reviews*, 46(1-3), 3–26. [https://doi.org/10.1016/s0169-409x\(00\)00129-0](https://doi.org/10.1016/s0169-409x(00)00129-0)
- [26] Mukhtar, M., Arshad, M., Ahmad, M., Pomerantz, R. J., Wigdahl, B., & Parveen, Z. (2008). Antiviral potentials of medicinal plants. *Virus research*, 131(2), 111–120. <https://doi.org/10.1016/j.virusres.2007.09.008>
- [27] Murugesu mudaliyar KS. *Siddha materia media (medicinal plants division)*. 8th ed. Chennai: Directorate of Indian Medicine & Homeopathy; 2006. p. 7e713.
- [28] Paliwa, J. K., Dwivedi, A. K., Singh, S., & Gupta, R. C. (2000). Pharmacokinetics and in-situ absorption studies of a new anti-allergic compound 73/602 in rats. *International journal of pharmaceutics*, 197(1-2), 213–220. [https://doi.org/10.1016/s0378-5173\(00\)00324-0](https://doi.org/10.1016/s0378-5173(00)00324-0)
- [29] Pires, D. E., Blundell, T. L., & Ascher, D. B. (2015). pkCSM: Predicting Small-Molecule Pharmacokinetic and Toxicity Properties Using Graph-Based Signatures. *Journal of medicinal chemistry*, 58(9), 4066–4072. <https://doi.org/10.1021/acs.jmedchem.5b00104>
- [30] Pitchiah Kumar, M.; Meenakshi Sundaram, K.; Ramasamy, M.S. Coronavirus Spike (S) Glycoprotein (2019-Ncov) Targeted Siddha Medicines Kabasura Kudineer and Thonthasura Kudineer In silico Evidence for Corona Viral Drug. *Asian J. Pharm. Res. Health Care* ; 1(12): 20-27, 2020. <https://doi.org/10.18311/AJPRHC/2020/25103>
- [31] Pop, R. M., Popolo, A., Trifa, A. P., & Stanciu, L. A. (2018). Phytochemicals in Cardiovascular and Respiratory Diseases: Evidence in Oxidative Stress and Inflammation. *Oxidative medicine and cellular longevity*, 2018, 1603872. <https://doi.org/10.1155/2018/1603872>
- [32] Prasanth, D., Murahari, M., Chandramohan, V., Panda, S. P., Atmakuri, L. R., & Guntupalli, C. (2020). In silico identification of potential inhibitors from Cinnamon against main protease and spike glycoprotein of SARS CoV-2. *Journal of biomolecular structure & dynamics*, 1–15. Advance online publication. <https://doi.org/10.1080/07391102.2020.1779129>

- [33] Salentin, S., Schreiber, S., Haupt, V. J., Adasme, M. F., & Schroeder, M. (2015). PLIP: fully automated protein-ligand interaction profiler. *Nucleic acids research*, 43(W1), W443–W447. <https://doi.org/10.1093/nar/gkv315>
- [34] Sarker, A.K., Ahamed, K.U., Chowdhury, J.U., & Begum, J.M. (2009). Characterization of an Expectorant Herbal Basak Tea Prepared with *Adhatoda vasica* Leaves. *Bangladesh Journal of Scientific and Industrial Research*, 44, 211-214. <https://doi.org/10.3329/bjsir.v44i2.3674>
- [35] Shahid M, Dar FK, Ismaeel AY, Al-Mahmeed A, Al Sindi K, Malik A, et al. Plant natural products as a potential source of antimicrobial agents: an overview and a glimpse on recent developments. *Recent trends in biotechnology and therapeutic applications of medicinal plants*. Dordrecht: Springer; 2013. p. 93e107.
- [36] Shaikh, S. A., Jain, T., Sandhu, G., Latha, N., & Jayaram, B. (2007). From drug target to leads--sketching a physicochemical pathway for lead molecule design in silico. *Current pharmaceutical design*, 13(34), 3454–3470. <https://doi.org/10.2174/138161207782794220>
- [37] Sinha, S. K., Shakya, A., Prasad, S. K., Singh, S., Gurav, N. S., Prasad, R. S., & Gurav, S. S. (2020). An in-silico evaluation of different Saikosaponins for their potency against SARS-CoV-2 using NSP15 and fusion spike glycoprotein as targets. *Journal of biomolecular structure & dynamics*, 1–12. Advance online publication. <https://doi.org/10.1080/07391102.2020.1762741>
- [38] Sutton, G., Fry, E., Carter, L., Sainsbury, S., Walter, T., Nettleship, J., Berrow, N., Owens, R., Gilbert, R., Davidson, A., Siddell, S., Poon, L. L., Diprose, J., Alderton, D., Walsh, M., Grimes, J. M., & Stuart, D. I. (2004). The nsp9 replicase protein of SARS-coronavirus, structure and functional insights. *Structure (London, England:1993)*, 12(2),341–353. <https://doi.org/10.1016/j.str.2004.01.016>
- [39] Thokchom P. Singh, Okram M. Singh and Huidrom B. Singh, “ *Adhatoda vasica* Nees: Phytochemical and Pharmacological Profile”, *The Natural Products Journal* (2011) 1: 29. <https://doi.org/10.2174/2210315511101010029>
- [40] Trott, O., & Olson, A. J. (2010). AutoDock Vina: improving the speed and accuracy of docking with a new scoring function, efficient optimization, and multithreading. *Journal of computational chemistry*, 31(2), 455–461. <https://doi.org/10.1002/jcc.21334>
- [41] UNNI, SRUTHI; Aouti, Snehal; Balasundaram, Padmanabhan (2020): Identification of a Potent Inhibitor Targeting the Spike Protein of Pandemic Human Coronavirus, SARS-CoV-2 by Computational Methods. *ChemRxiv*. Preprint. <https://doi.org/10.26434/chemrxiv.12197934.v1>
- [42] Veeresham C. (2012). Natural products derived from plants as a source of drugs. *Journal of advanced pharmaceutical technology & research*, 3(4), 200–201. <https://doi.org/10.4103/2231-4040.104709>
- [43] Wadood, Abdul & Ahmed, N & Shah, L & Ahmad, Ayaz & Hassan, Hammad & Shams, Sulaiman. (2013). In-silico drug design: An approach which revolutionised the drug discovery process. *OA Drug Design and Delivery*. 1. 10.13172/2054-4057-1-1-1119
- [44] Wagner H. (1989). Search for new plant constituents with potential antiphlogistic and antiallergic activity. *Planta medica*, 55(3), 235–241. <https://doi.org/10.1055/s-2006-961992>
- [45] Wallace, A. C., Laskowski, R. A., & Thornton, J. M. (1995). LIGPLOT: a program to generate schematic diagrams of protein-ligand interactions. *Protein engineering*, 8(2), 127–134. <https://doi.org/10.1093/protein/8.2.127>
- [46] Webster, D., Taschereau, P., Lee, T. D., & Jurgens, T. (2006). Immunostimulant properties of *Heracleum maximum* Bartr. *Journal of ethnopharmacology*, 106(3), 360–363. <https://doi.org/10.1016/j.jep.2006.01.018>
- [47] wenzhong, liu; hualan, Li (2020): COVID-19 Disease: ORF8 and Surface Glycoprotein Inhibit Heme Metabolism by Binding to Porphyrin. *ChemRxiv*. Preprint. <https://doi.org/10.26434/chemrxiv.11938173.v3>

aFigures

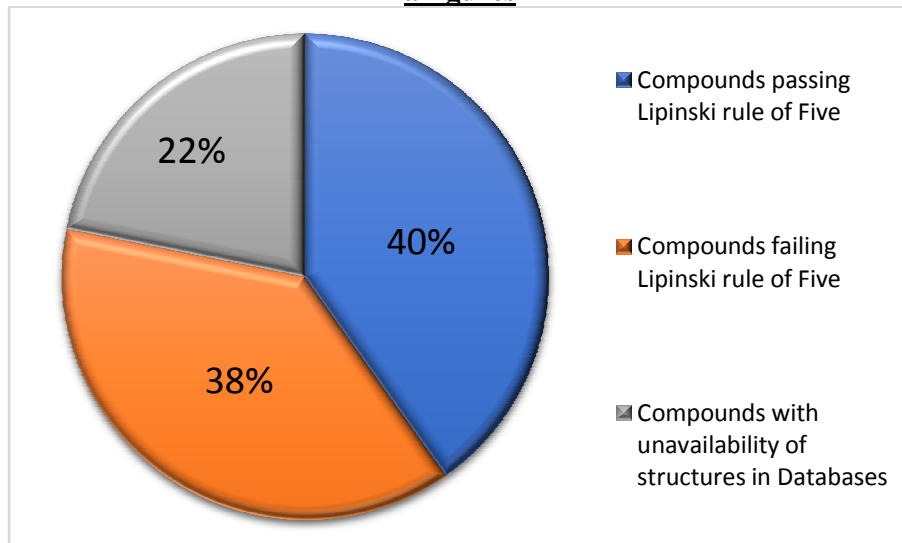
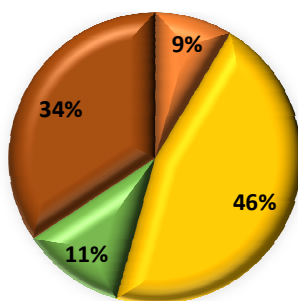


Figure 1: Summary of ADME passed phytocompounds from *J. Adhatoda*



- Ligands that failed to satisfy docking score threshold
- Ligands that failed AMES test
- Ligands that failed hepatotoxicity test
- Ligands with good docking score and toxicity profile

Figure 2: Selection of phytochemicals based on docking score (< -7 kcal/mol) and toxicity analysis

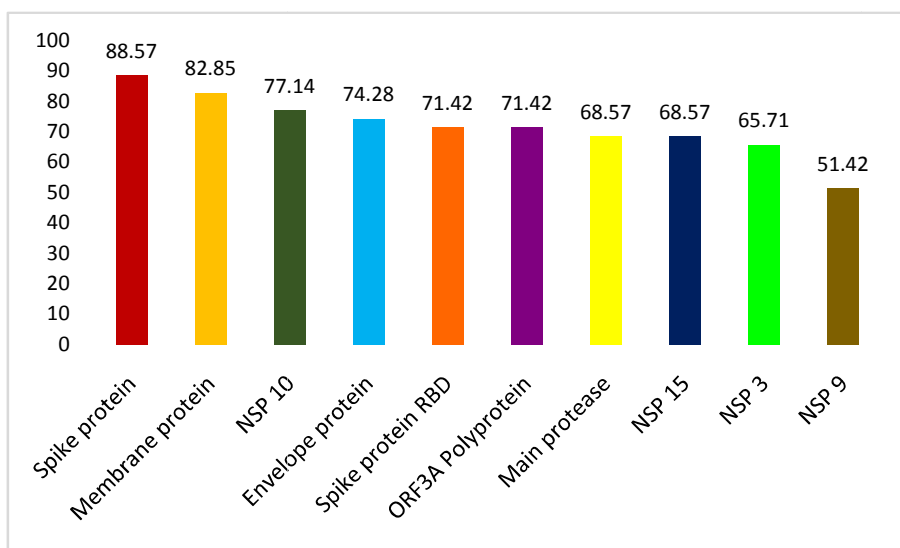
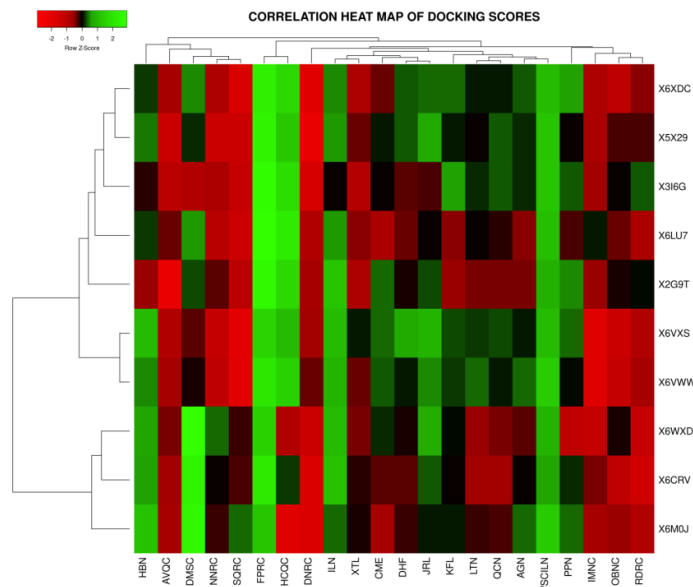
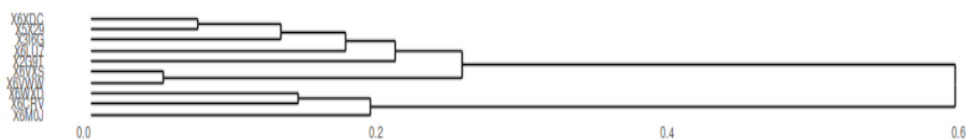


Figure 3: Percentage of phytochemicals showing binding affinity lesser than -7 kcal/mol against SARS-CoV-2 proteins



Row Dendrogram



Column Dendrogram

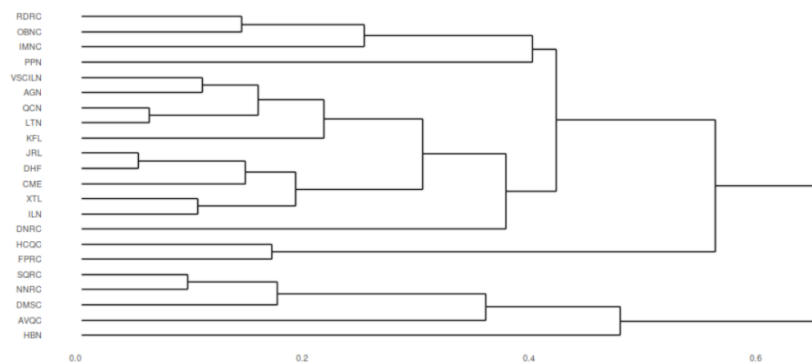


Figure 4: Correlation heat map (Average linkage, Pearson's distance measurement, Scale type: row) generated by Heat mapper online tool for the docking scores of the 12 ligands and 10 FDA approved drugs with the 10

protein targets of SARS-CoV-2. The left vertical axis represents the SARS-CoV-2 targets: X6CRV: Spike Protein, X5X29: Envelope Protein, X3I6G: Membrane Protein, X6LU7: Main Protease, X6M0J: Spike Protein RBD, X6XDC: ORF3a Polyprotein, X6WXD: Nsp3, X2G9T: Nsp9, X6VWW: Nsp10, X6VXS: Nsp15. The horizontal axis represents the 10 FDA approved drugs as positive control followed by 12 ligands: AVQC: Atovaquone, DNRC: Darunavir, DMSC: Dexamethasone, FPRC: Favipiravir, HCQC: Hydroxychloroquine, IMNC: Ivermectin, NNRC: Nelfinavir, OBNC: Ouabain, RDRC: Remedevsir, SQRC: Saquinavir, DHF: 3',4'-Dihydroxyflavonol, APG: Apigenin, CME: Chinensinaphthol methyl ether, HBN: Heliobupthalmin, ILN: Isolariciresinol, JRL: Justiciresinol, KFL: Kaempferol, LTN: Luteolin, PPN: Podophyllotoxin, QCN: quercetin, VSCILN: Vasicilonone, XTL: Xanthoxylol.

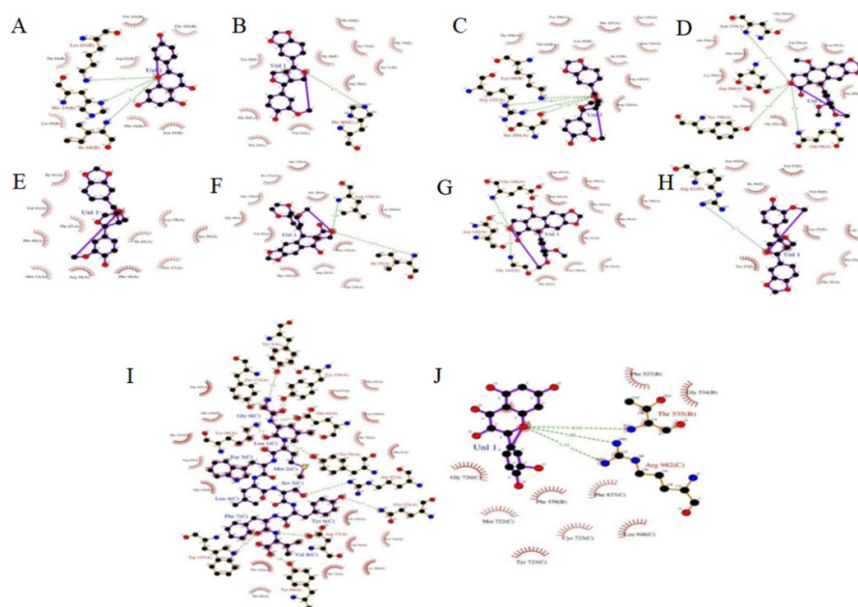
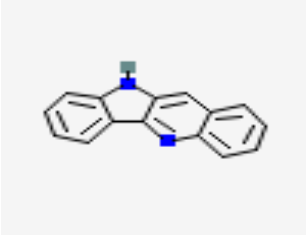
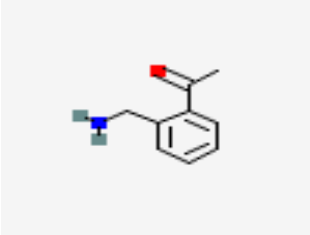
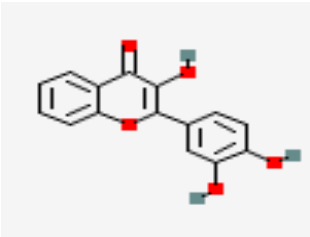
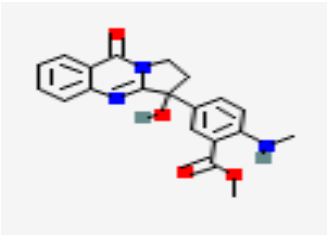
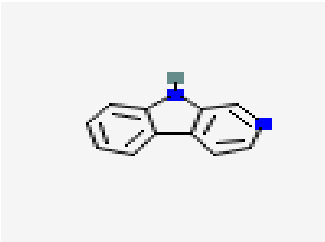
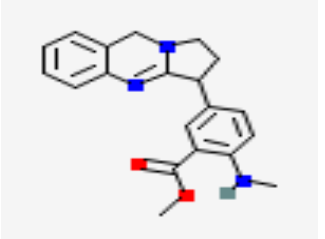
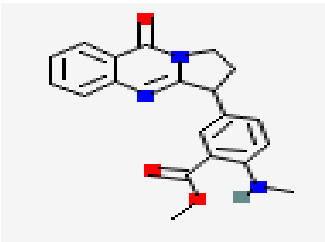
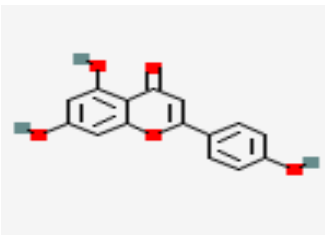
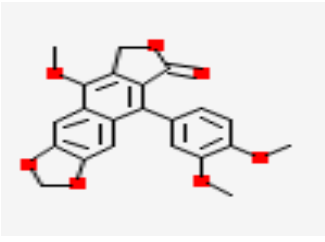


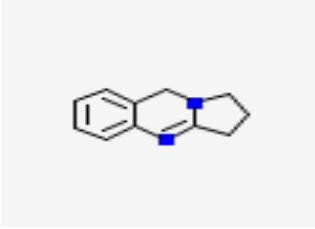
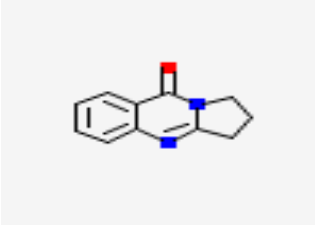
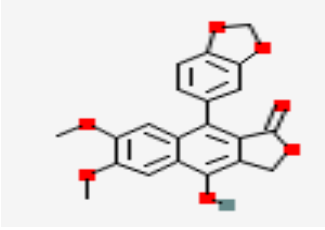
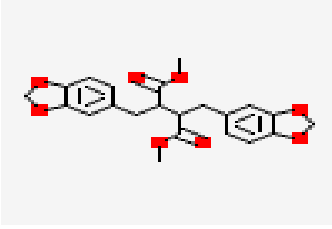
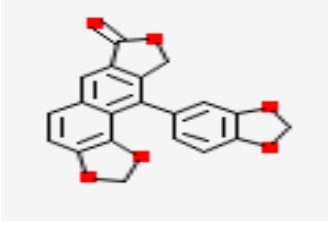
Figure 5: 2D Ligand interaction profile using LIGPLOT: A) Nsp15(6VXS)-Apigenin B) Nsp10(6VWW)-Xanthoxylol C) ORF3a Polyprotein(6XDC)-Xanthoxylol D) Spike Protein Receptor Binding Domain (6M0J)-Chinensinaphthol methyl ether E) Nsp9(2G9T)-Xanthoxylol F) Nsp3(6WXD)-Podophyllotoxin G) Main Protease(6LU7)-Chinensinaphthol methyl ether H) Envelope Protein(5X29)-Xanthoxylol I) Membrane Protein(3I6G)-Xanthoxylol J) Spike Protein(6CRV)-Quercetin

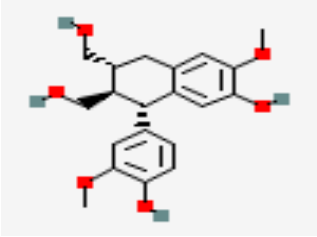
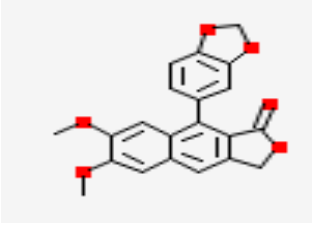
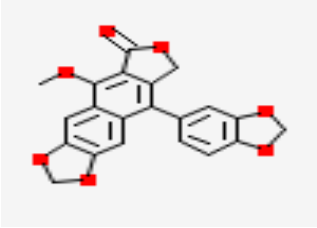
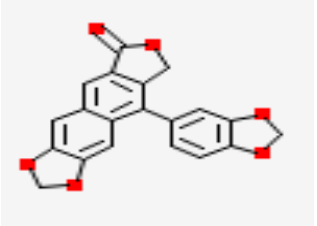
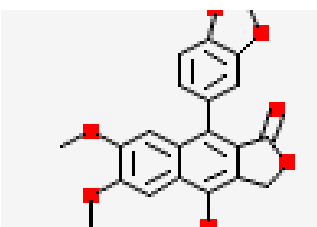
Tables

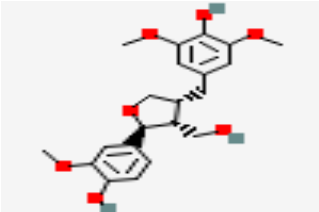
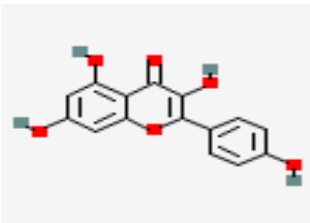
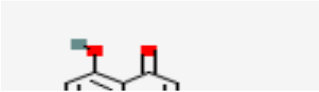
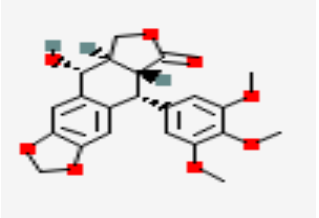
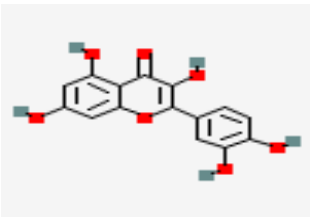
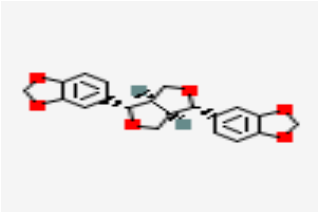
Table 1: Phytocompounds from *J. adhatoda* and FDA approved repurposed drugs

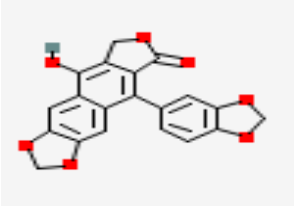
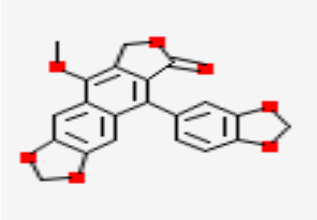
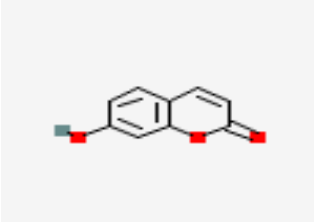
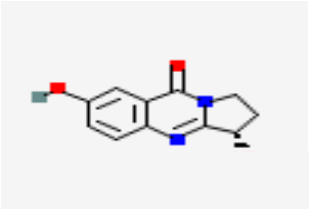
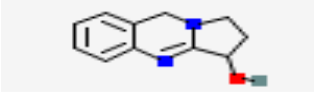
S · N	Compound	Source/ID	Structure	Pharmacological function	References
	10H-quindoline	PubChem 98912		Anticancer activity and cellular repression of c-MYC	https://pubmed.ncbi.nlm.nih.gov/22691117/
	2-acetylbenzylamine	PubChem 22379528		Anticancer activity	https://doi.org/10.1016/j.biopha.2017.06.096
	3',4'-dihydroxyflavonol	PubChem 145826		Antioxidant, prevents diabetes and vasodilator	Jimenez et al., 2001; Wang et al., 2004; Woodman et al., 2005; Woodman & Malakul, 2009
	3-hydroxyanisoline	PubChem 101670821		Antibacterial activity	DOI: 10.3329/dujs.v60i1.10326 Neoandrographolide Isolated from leaves of <i>Adhatoda vasica</i>

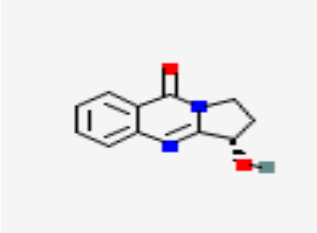
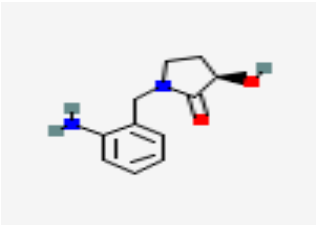
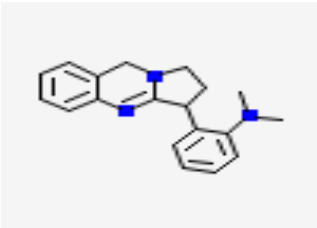
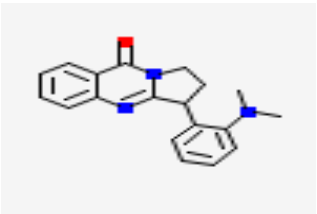
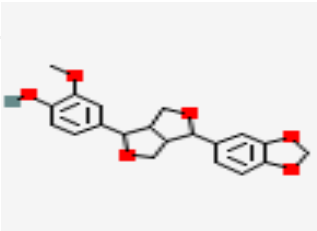
9-acetamido-3,4-dihydropyridino-(3,4-b)	PubChem 64961		Neurotherapeutic for cocaine related disorders	https://pubmed.ncbi.nlm.nih.gov/11418284/
Adhatodine	PubChem 52908915		Antimalarial	https://pubmed.ncbi.nlm.nih.gov/26142781/
Anisotine	PubChem 442884		anti-tuberculosis activity	Appl Biochem Biotechnol . 2012 Nov;168(5):980-90. doi: 10.1007/s12010-012-9834-1. Epub Wahi et al.. 1974: Sawatzky et al.. 2006: Cai et al., 2011
Apigenin	PubChem 5280443		Anti-inflammatory and anti-tumor	Day et al.. 1999
Chinensinaphthol methyl ether	PubChem 5315828		Antiplatelet aggregation	

Deoxyvasicine	PubChem 442894		cholinesterase and selective MAO-A inhibitor	https://pubmed.ncbi.nlm.nih.gov/18560630/
Deoxyvasicineone	PubChem 68261		anti-microbial, anti-inflammatory and antidepressant activities	Koizumi, M.; Matsuura, I.; Murakami, Y. Japan Kokai, 1977, 093, 7777; Chem. Abstr. 1978, 88, Arch Pharm (Weinheim) . 2012 Aug;345(8):622-8. doi: 10.1002/ardp.201200035. Epub 2012 Day et al.. 1999; Duarte et al.. 2010
Diphyllin	PubChem 100492		Anticancer activity	
Heliobuphthalmine	PubChem 75229604		Antineoplastic	
Helioxanthin	PubChem 177023		Inhibition human hepatitis B viral replication and antitumor	Chang et al.. 2000; Tseng et al.. 2008

Isolaric iresinol	PubChem 160521		Anti- inflammatory	Kupeli et al., 2003
Justici din B	PubChem 442882		Anti- inflammatory, antiplatelet aggregation, cytotoxicity, antiviral, fungicidal.	Baba et al. 1996; Catch et al., 2003; Kavitha et al., 2003; Rao et al.. 2006; Wu et al.. 2007; Kaur et at, 2009
Justici din D	PubChem 5318737		Antiplatelet aggregation	Fukamiya & Lee. 1986; Chen et al., 1996; Wu et al., 2007 Fukamiya & Lee, 1986; Asano et al.. 1996
Justici din E	PubChem 363128		inhibitor of leukotriene biosynthesis by human leukocytes	https://doi.org/10.1016/S0960-894X(01)81016-7
Justici din A	PubChem 159982		Anti-cancer activity, Cytotoxic activities against hepatocellular carcinoma,	https://doi.org/10.1007/s11064-016-1857-5 https://doi.org/10.1007/s00044-009-9172-1

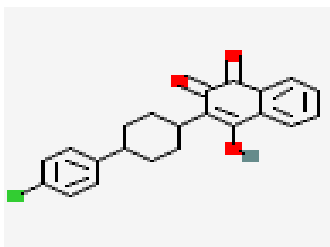
Justicir esinol	PubChem 131934		Cytotoxicity	https://doi.org/10.1021/np50078a023
Kaempferol	PubChem 5280863		Flavonoid kaempferol is known to suppress growth of several human malignancies	https://doi.org/10.1158/1535-7163.mct-06-0788 https://doi.org/10.1016/j.jss.2008.02.036
Luteolin	PubChem 5280445		Potential anti-oxidant, anti-inflammatory	https://ncit.nci.nih.gov/ncitbrowser/ncicentreport.jsp?doi=10.1016/s0031-9422(00)00094-7
Podophyllotoxin	PubChem 10607		Cancer chemotherapy	
Quercetin	PubChem 5280343		Treat or prevent diverse conditions including cardiovascular disease, hypercholester	https://www.ncbi.nlm.nih.gov/books/nbk556474/
Sesamin	PubChem 72307		Angiogenic	http://dx.doi.org/10.15562/phytoedicine.2019.93

Taiwan in E	PubChem49 3164		Antiplatelet aggregation and antitumor	https://doi.org/10.1021/np960443+ https://doi.org/10.1016/s0031-9422(00)00275-2
Taiwan in E methyl ether	PubChem 11740369		Antiplatelet aggregation and cytotoxicity against human cervical carcinoma Anti- inflammatory, antinociceptive , and bronchodilator activities. Treatment of respiratory diseases	http://dx.doi.org/10.15562/phytomedicine.2019.93 https://doi.org/10.1021/np9900167 https://doi.org/10.1021/np960443+ https://doi.org/10.1590/s0102-695x2011005000196
Umbelliferone	PubChem 5281426			
Vasicinolone	PubChem 158720		anti- inflammatory and antimicrobial	https://pubmed.ncbi.nlm.nih.gov/23357363/
Vasicinone	PubChem 72610		Treatment of bronchitis	https://doi.org/10.1021/jo01037a041

Vasicinone	PubChem 442935		Treatment of bronchitis, Potential candidate for the treatment of Parkinson's disease and	https://doi.org/10.1021/jo01037a041 https://doi.org/10.3390/nu11071655
Vasicolin	PubChem 92470596		Hepatoprotective activity	Sharma, ajay & bhardwaj, garima & cannoo, damanjit. (2018). Overview of phytochemistry and pharmacology https://doi.org/10.1016/s0099-9598(08)60247-3
Vasicoline	PubChem 626005		Anticholinesterase activity	
Vasicolinone	PubChem 130679		anti-tuberculosis activity	Appl Biochem Biotechnol . 2012 Nov;168(5):980-90. doi: 10.1007/s12010-012-9834-1. Epub https://doi.org/10.1248/bpb.16.930
Xanthoxylol	130679 PubChem 130679		Antitumor effect on mouse, skin, and pulmonary carcinogenesis	http://dx.doi.org/10.15562/phytochemistry.2019.93

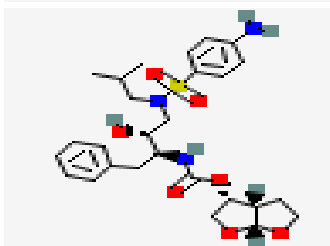
FDA Approved Repurposed COVID 19 Drugs

Atovaquone PubChem
74989



Antimalarial and Anticancer activity

Darunavir PubChem
213039



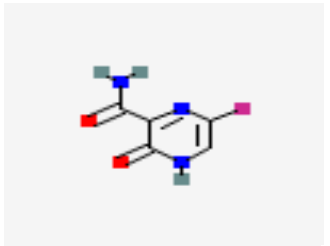
Human immunodeficiency virus type 1 (HIV-1) protease nonpeptidic inhibitor

Dexamethasone PubChem
5743



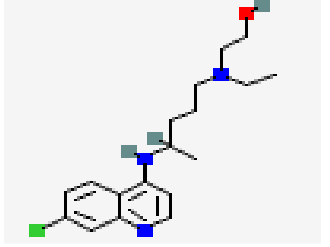
Anti-inflammatory and Anti-cancer

Favipiravir PubChem
492405



Antiviral

Hydroxychloroquine PubChem
3652



Anti-inflammatory, Anti-tumor and Anti-malarial

doi:
10.1038/s41467-017-02603-z
Oncotarget. 2016 Jun 7; 7(23): 34084–34099. Published online
Ghosh AK et al
Potent HIV protease inhibitors incorporating high-affinity p2-ligands and (r)-(hydroxyethylamino)
doi:
10.3390/ijms21072605
PMCID: PMC7177823
PMID: 32283655
Anti-2018 Mar 27;15(3):e1002535. doi:
10.1371/journal.pmed.1002535. eCollection 2018 Mar.
PMID 31268153; International journal of oncology 2019 Aug; 55(2):405-414
PMID 29981383;

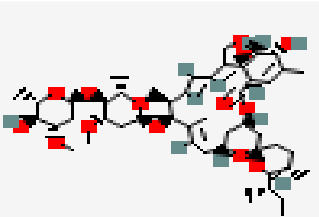
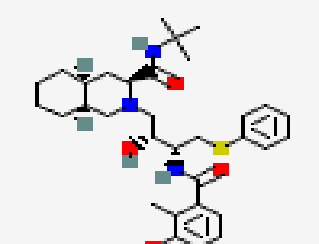
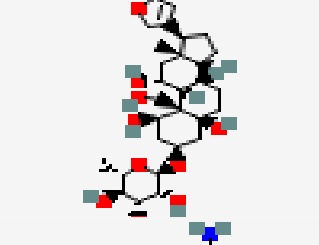
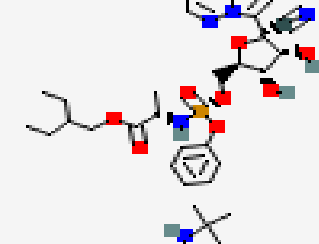
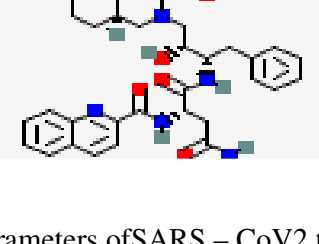
Ivermectin	PubChem 6321424		Antiparasitic	doi: 10.5455/2319-2003.ijbcp002712 Ivermectin: pharmacology and therapeutic applications doi: 10.2147/DDDT.S 102241 PMCID: PMC4898046
Nelfinavir	PubChem 64143		Anticancer, Antiviral, Anti- HIV	doi: 10.1128/AAC.45. 4.1086-1093.2001 doi: 10.3390/ijms2009 2111 PMCID: PMC6539428
Ouabain	PubChem 439501		Enhances cell- cell adhesion, cell migration	doi: 10.1371/journal.p https://doi.org/10.1016/j.dsx.2020.05.018
Remdesivir	Pubchem 121304016		Antiviral	Remdesivir in COVID-19: A critical review of pharmacology, doi: 10.2165/00003088 -199834030- 00002.
Saquinavir	Pubchem 441243		HIV protease inhibitor	Saquinavir. Clinical pharmacology and

Table 2: Grid parameters of SARS – CoV2 target proteins

S.No	Protein	PDB ID	xyz coordinates of grid center (□)	xyz coordinates	Spacing (□)
------	---------	-----------	---------------------------------------	--------------------	----------------

				of grid size (□)	
1	Spike protein	6CRV	162.996,164.796,153.525	82,82,90	1.000
2	Envelope protein	5X29	5.513, -0.464,6.602	40,40,40	0.503
3	Membrane protein	3I6G	26.338,1.956,45.596	40,40,40	0.503
4	Protease	6LU7	-11.028,14.333,68.191	40,40,40	0.500
5	Spike protein receptor binding domain	6MOJ	-26.827,18.465, -9.269	30,50,88	1.000
6	ORF 3a	6XDC	145.801,145.378,153.392	40,40,40	0.500
7	Non structural protein 3 (Nsp3)	6WXD	5.513,0.464,6.602	40,40,40	0.503
8	Non structural protein 9 (Nsp9)	2G9T	56.325,1.573,21.494	40,40,40	0.500
9	Non structural protein 10 (Nsp10)	6VWW	119.130,121.902,81.992	76,82,126	1.000
10	Non structural protein 15 (Nsp15)	6VXS	-69.046,26.670, -0.197	56,58,52	0.878

Table 3: Lipinski rule of five parameters for the selected phytochemicals

S.No.	Compound	Formula	MW	Log P				Silico s-ITlogP	Consensus logP	H-bond acceptor
				ilogP	XlogP3	WlogP	MlogP			

	10h-quindoline	C15H 10N2	218.2 5	2.02	3.74	3.87	3.04	4.05	3.35	1
	2-acetyl benzyl amine	C19H 19N3 O	305.3 7	2.86	2.76	3	3.26	2.87	2.95	2
	3',4'- dihydroxyflavono l	C9H6 O3	162.1 4	1.44	1.58	1.5	1.04	1.97	1.51	3
	3- hydroxyanisotine	C20H 19N3 O4	365.3 8	2.69	2.26	1.57	2.05	2.39	2.19	5
	9-acetamido- 3,4dihydropyrido -(3,4-b) indole	C11H 8N2	168.1 9	1.43	3.17	2.72	1.62	3.09	2.41	1
	Adhatodine	C11H 10N2 O2	202.2 1	1.67	0.52	0.51	0.78	1.23	0.94	3
	Anisotine	C20H 19N3 O3	349.3 8	3.21	3.02	2.57	2.85	2.89	2.91	4
	Apigenin	C15H 10O5	270.2 4	1.89	3.02	2.58	0.52	2.52	2.11	5
	Chinensinaphthol methyl ether	C22H 18O7	394.3 7	3.37	3.95	3.78	2.29	4.7	3.62	7
l.	Deoxyvasicine	C11H 13Cl N2	208.6 9	0	1.8	2.21	2.73	2.75	1.9	1
..	Deoxyvasicinone	C11H 10N2 O	186.2 1	2.09	1.07	1.34	2.04	2.16	1.74	2
l.	Diphyllin	C21H 16O7	380.3 5	2.84	3.62	3.48	2.07	4.16	3.23	7
l.	Heliobupthalmin	C22H 22O8	414.4 1	3.98	3.48	2.51	2.3	4.12	3.28	8
l.	Helioxanthin	C20H 12O6	348.3 1	2.99	3.85	3.48	2.52	4.41	3.45	6
l.	Isolariciresinol	C20H 24O6	360.4	2.37	2.05	2.02	1.17	2.53	2.03	6
l.	Justicidin A	C22H 18O7	394.3 7	3.4	3.95	3.78	2.29	4.7	3.62	7

4.	Justicidin B	C21H 16O6	364.3 5	3.15	3.98	3.77	2.34	4.64	3.58	6
5.	Justicidin D	C21H 14O7	378.3 3	3.22	3.82	3.49	2.48	4.44	3.49	7
6.	Justicidin E	C20H 12O6	348.3 1	3.1	3.85	3.48	2.52	4.41	3.47	6
7.	Justiciresinol	C21H 26O7	390.4 3	3.04	2.37	2.34	0.86	2.93	2.31	7
8.	Kaempferol	C15H 10O6	286.2 4	1.7	1.9	2.28	-0.03	2.03	1.58	6
9.	Luteolin	C15H 10O6	286.2 4	1.86	2.53	2.28	-0.03	2.03	1.73	6
10.	Podophyllotoxin	C22H 22O8	414.4 1	3.25	2.01	2.08	1.43	2.9	2.33	8
11.	Quercetin	C15H 10O6	286.2 4	1.7	1.9	2.28	-0.03	2.03	1.58	6
12.	Sesamin	C20H 18O6	354.3 5	3.46	2.68	2.57	1.98	3.25	2.79	6
13.	Taiwanin E	C20H 12O7	364.3 1	2.79	3.49	3.19	2.26	3.92	3.13	7
14.	Taiwanin E methyl ether	C21H 14O7	378.3 3	3.27	3.82	3.49	2.48	4.44	3.5	7
15.	Umbelliferone	C9H6 O3	162.1 4	1.44	1.58	1.5	1.04	1.97	1.51	3
16.	Vasicine	C11H 12N2 O	188.2 3	1.94	0.44	0.38	1.57	1.8	1.23	2
17.	Vasicinolone	C11H 10N2 O3	218.2 1	1.53	0.03	0.21	0.63	0.72	0.62	4
18.	Vasicinone	C11H 10N2 O2	202.2 1	1.67	0.52	0.51	0.78	1.23	0.94	3
19.	Vasicol	C11H 14N2 O2	206.2 4	1.44	0.05	-0.16	0.32	0.68	0.46	2
20.	Vasicoline	C19H 21N3	291.3 9	2.79	2.81	2.87	3.63	3.42	3.11	1
21.	Vasicolinone	C19H 19N3	305.3 7	2.86	2.76	3	3.26	2.87	2.95	2

i.	Xanthoxylol	O C ₂₀ H 20O ₆	356.3 7	3.25	2.48	2.56	1.57	2.96	2.56	6
----	-------------	--	------------	------	------	------	------	------	------	---

MW – Molecular Weight **MR** – Molar Refractivity

Table 4: Toxicity profile for the lead molecules

S	Compound	AMES toxicity	Max. tolerated dose (log mg/kg/day)	hERG I inhibitor	hERG II inhibitor	Oral Rat Acute Toxicity (LD50) (mol/kg)	Oral Rat Chronic Toxicity (LOAEL) (log mg/kg_bw/day)	He patotoxicity	Skin sensitization	T.P or mis toxicity (log ug/L)	Min now toxicity (log mM)
1.	3',4'-Dihydroxyflavonol	No	0.314	No	No	1.99	2.592	No	No	0.27	1.748
2.	Apigenin	No	0.337	No	No	1.978	1.959	No	No	0.517	1.17
3.	Chinensinapht hol Methyl Ether	No	0.307	No	Yes	3.053	0.73	No	No	0.288	-0.975
4.	Heliobuphth almin	No	0.489	No	No	2.747	1.476	No	No	0.286	-0.631
5.	Isolariciresinol	No	-0.019	No	Yes	2.003	1.947	No	No	0.432	2.332
6.	Justiciresinol	No	0.276	No	No	2.109	1.519	No	No	0.453	1.661

7.	Kaempferol	No	0.531	No	No	2.449	2.505	No	No	0.312	2.885
8.	Luteolin	No	0.564	No	No	2.453	1.537	No	No	0.428	1.346
9.	Podophyllotoxin	No	-0.45	No	No	2.512	1.037	No	No	0.292	-0.199
10	Quercetin	No	0.499	No	No	2.471	2.612	No	No	0.288	1.301
11	Vasicilonone	No	0.246	No	No	1.813	1.331	No	No	0.556	1.723
12	Xanthoxylol	No	-0.583	No	Yes	2.211	1.479	No	No	0.43	0.767

Table 5: Docking scores of phytochemicals against SARS-CoV-2 target proteins

S. No.	Molecule/target protein	Binding energy (kcal/mol)									
		Spike protein	Envelope protein	Membrane protein	Protease	Spike protein receptor binding domain	ORF3a	NSP3	NSP9	NSP10	NSP15
	3',4'-Dihydroxyflavonol	-8.8	-7.5	-8.9	-7.7	-8.3	-7.5	-7.3	-7	-8.3	-7.3

Apigenin	-8.5	-7.7	-8.4	-7.8	-7.7	-7.5	-7.5	-7.3	-8	-8
Chinensinaphthol methyl ether	-8.8	-7.8	-8.6	-8	-8.8	-8.2	-7.1	-6.6	-8.1	-7.7
Heliobupthalamin	-7.8	-7.3	-8.7	-7.2	-6.9	-7.6	-6.7	-7.4	-7.9	-6.9
Isolariciresinol	-7.2	-7.2	-8.6	-6.9	-7.7	-7.3	-6.4	-5.9	-7.5	-6.9
Justiciresinol	-8.1	-7	-8.8	-7.4	-8	-7.4	-6.6	-6.7	-7.9	-7.1
Kaempferol	-8.5	-7.8	-7.9	-7.8	-8	-7.4	-7.2	-7.4	-8.2	-7.8
Luteolin	-9.1	-7.9	-8.4	-7.4	-8.3	-7.7	-7.7	-7.3	-8	-7.9
Podophyllotoxin	-8.3	-7.9	-8.2	-7.6	-7.7	-7.2	-8.1	-6.5	-8.4	-7.7
Quercetin	-9.1	-7.5	-8.2	-7.5	-8.4	-7.7	-7.6	-7.3	-8.3	-7.8
Vasicilonone	-7.7	-6.4	-7.3	-6.4	-6.7	-6.8	-6.5	-6.2	-7	-6.9
Xanthoxylol	-8.6	-8.4	-9.5	-7.8	-8.2	-8.6	-7.6	-7.6	-8.8	-8

Table 6: Docking binding affinity of FDA approved repurposed drugs against SARS-CoV 2 target proteins

Docking Binding Affinity (kcal/mol)

S. No.	Positive controls	Spike protein	Envelope protein	Membrane protein	Protease	Spike protein receptor binding domain	ORF3a	NSP3	Nsp9	Nsp10	Nsp15
1	Atovaquone	-9.1	-9.6	-9.6	-7.7	-8.8	-8.5	-7.6	-8.8	-9.1	-9.1
2	Darunavir	-10.3	-10.6	-10.2	-8.1	-9.9	-9.7	-8.3	-7.5	-8.8	-8.8
3	dexamethasone	-5.8	-7.7	-9.4	-6.9	-5.3	-7.3	-4.9	-6.7	-8.5	-8.5
4	Hydroxychloroquine	-8.2	-6.3	-6.7	-5.4	-10.1	-6.1	-7.9	-5.5	-6.9	-6.9
5	ivermectin	-8.9	-8.8	-9.2	-7.3	-8.8	-8.6	-8.2	-7.4	-10.3	-10.3
6	Nelfinavir	-8.5	-9.6	-9.3	-8.2	-8.3	-8.6	-6.9	-7.2	-9.5	-9.5
7	Ouabain	-9.6	-8.2	-8.6	-7.7	-8.7	-8.9	-7.3	-7	-9.6	-9.6
8	remedevsir	-10	-8.2	-8.2	-8	-9	-8.3	-8.2	-6.9	-9.1	-9.1
9	Saquinavir	-8.7	-9.6	-9.8	-8.6	-7.7	-9.5	-7.4	-7.8	-10.4	-10.4
1	Favipiravir	-6.1	-4.7	-5.6	-4.8	-6.8	-5.4	-6	-4.6	-6.3	-4.9

Table 7: Protein-ligand interaction of top-scoring compounds

S. No.	Protein	PDB ID	Ligand	Binding affinity (kcal/mol)	Amino acid residues involved and distance (Å)	
					Hydrogen bonding	Hydrophobic interactions
1	Spike protein	6CRV	Quercetin	-9.1	535B THR (1.97), 722C MET (1.93), 727C ASP (2.30), 957C SER (3.32), 959C LEU (2.93), 960C ASN (2.70), 982C ARG (1.97), 982C ARG (2.26)	558B PHE (3.59), 558B PHE (3.75), 837C PHE (4.00), 948C LEU (3.93)
2	Envelope protein	5X29	Xanthoxylol	-8.4	35A THR (3.36), 35A THR (3.13), 61D ARG (3.26), 61D ARG (2.65), 64D ASN (2.94), 64D ASN (2.37)	31A LEU (3.89), 47E VAL (3.57), 49E VAL (3.70), 57E TYR (3.62), 57E TYR (3.57), 57E TYR (3.77), 57E TYR (3.77)

3	Membrane protein	3I6 G	Xanthoxylol	- 9.5	26B TYR (1.82), 52B SER (3.39), 67B TYR (2.23)	63B TYR (3.91), 65B LEU (3.87), 235A PRO (3.76)
4	Main protease	6L U7	Chinensinaphthol methyl ether	-8	26A THR (2.98), 143A GLY (2.28), 166A GLU (2.15)	165A MET (3.81)
5	Spike protein receptor binding domain	6 M 0J	Chinensinaphthol methyl ether	- 8.8	98A GLN (2.23), 196A TYR (3.09), 196A TYR (2.38), 205A GLY (3.05), 206A ASP (3.27), 210A ASN (2.24), 562A LYS (2.49)	95A LEU (3.67), 102A GLN (3.63), 210A ASN (3.77)
6	ORF 3a	6X D C	Xanthoxylol	- 8.6	66B LYS (2.28), 122A ARG (2.22), 122A ARG (1.97), 205A SER (1.91)	206A TYR (3.52), 206A TYR (3.67), 207A PHE (3.96), 207A PHE (3.63)
7	Nsp 3	6 W X D	Podophyllotoxin	- 8.1	23A ILE (2.18), 126A LEU (2.27)	23A ILE (3.63), 126A LEU (3.74), 156A PHE (3.58),

						160A LEU (3.95)
8	Nsp 9	2G 9T	Xanthoxylol	- 7.6	59A SER (1.95)	40A PHE (3.68), 56A PHE (3.46), 65A ILE (3.95)
9	Nsp 10	6V W W	Xanthoxylol	- 8.8	18L ALA (3.16), 80E HIS (2.31)	71E ALA (3.50)
1 0	Nsp 15	6V XS	Apigenin	-8	15B HIS (2.46), 64B ILE (2.42), 102B VAL (2.02)	102B VAL (3.80)

Table 8 Binding interaction of protein-ligand complexes against SARS-CoV 2 target proteins

S.No.	Protein-phyto compound complex	Binding affinity (kcal/mol)	Protein-drug complex	Binding affinity (kcal/mol)	Common amino acid residues shared by phytocompounds and FDA approved COVID drugs	
					Hydrogen bonding	Hydrophobic interactions
1	Membrane protein-Xanthoxylol	-9.5	Membrane protein-Darunavir	-10.3	26B TYR	63B TYR, 235A PRO
4	Main protease-Chinensinaphthol methyl	-8	Main protease-Saquinavir	-8.6	143A GLY, 166A GLU	165A MET

5	ether Spike protein receptor binding domian- Chinensinap thol methyl ether	-8.8	Spike protein receptor binding domian- Hydroxychloro quine	-10.1	-	95A LEU, 210A ASN
7	Nsp 3- Podophyllot oxin	-8.1	NSP 3- Darunavir	-8.3	-	23A ILE, 126A LEU, 156A PHE, 160A LEU 40A PHE, 56A PHE
8	Nsp 9- Xanthoxylol	-7.6	NSP 9- Atovaquone	-8.8	-	

Table 9: ADME/T properties of the screened phytocompounds

S. N O.	COMPOUND	ABSORPTION		DISTRIBUTION	METABOLISM		EXCRETION	TOXICITY	
		Water solubility	Intestinal absorption (human)	BBB Permeability	CY P3 A4 substrate	CY P3 A4 inhibitor	Total clearance	Max Tolerated dose (human)	Oral rat acute toxicity
1.	3',4'-	-	94.8	-0.199	No	No	0.731	0.31	1.9

	dihydroxyflavonol	1.1 37	75					4	9
2.	Apigenin	- 3.3 8	91.5 66	-0.903	No	No	0.595	0.33 7	1.9 78
3.	Chinensinaphthol methyl ether	- 4.7 16	100	-0.961	Yes	No	0.461	0.30 7	3.0 53
4.	Heliobuphthalm in	- 4.6 63	100	-1.118	Yes	Yes	0.057	0.48 9	2.7 47
5.	Isolariciresinol	- 3.0 4	74.2 9	-0.939	No	No	0.477	0.53 1	2.4 49
6.	Justiciresinol	- 4.6 18	71.7 91	-1.038	Yes	Yes	0.176	0.27 6	2.1 09
7.	Kaempferol	- 3.2 82	80.0 64	-1.065	No	No	0.496	0.77 4	2.1 97
8.	Luteolin	- 3.2 94	82.1 75	-1.145	No	Yes	0.568	0.56 4	2.4 53
9.	Podophyllotoxin	- 3.9 71	100	-0.821	Yes	Yes	0.205	- 0.45	2.5 12
10.	Quercetin	- 3.2 82	80.0 64	-1.065	No	No	0.496	0.77 4	2.1 97
11.	Vasicilonone	- 2.9 25	77.2 07	-1.098	No	No	0.407	0.49 9	2.4 71
12.	Xanthoxylol	- 3.6 88	94.7 56	-0.578	Yes	Yes	- 0.046	- 0.58 3	2.2 11

Table 10: Prediction of Activity Spectra for Substances (PASS) for lead compounds

S.No.

Compound

Antiviral

	Adeno Virus		HIV		Influenza		Hepatitis B	
	Pa	Pi	Pa	Pi	Pa	Pi	Pa	Pi
1. 3',4'-Dihydroxyflavonol	0.259	0.128	0.184	0.038	0.291	0.095	0.416	0.013
2. Apigenin	0.301	0.088	0.135	0.085	0.459	0.030	0.469	0.007
3. Chinensinaphthol methyl ether	0.228	0.167	-	-	0.204	0.191	0.206	0.046
4. Heliobuphthalmol	0.339	0.060	0.225	0.021	0.253	0.128	0.172	0.130
5. Isolariciresinol	0.216	0.184	-	-	0.262	0.120	0.255	0.049
6. Justiciresinol	-	-	0.200	0.030	0.332	0.072	0.276	0.040
7. Kaempferol	0.246	0.143	0.164	0.051	0.400	0.047	0.496	0.005
8. Luteolin	0.246	0.143	0.149	0.067	0.462	0.030	0.437	0.006
9. Podophyllotoxin	-	-	-	-	0.209	0.183	0.190	0.099
10. Quercetin	-	-	0.170	0.047	0.403	0.046	0.498	0.005
11. Vasicilonone	-	-	0.308	0.236	0.206	0.189	-	-
12. Xanthoxylol	0.290	0.097	-	-	0.422	0.040	0.228	0.063

Pa- Probability of molecule to be active; **Pi-** Probability of molecule to be inactive

Supplementary information

Table S1: List of phytochemicals from *Justicia adhatoda*

S.No.	Name of phytochemicals
1.	Vasicine
2.	Vasicinone
3.	adhatodine
4.	Vasicinolone
5.	vasicol
6.	vasicoline
7.	vasicolinone
8.	2-acetyl benzyl amine
9.	Anisotine
10.	β -sitosterol
11.	tritricontane
12.	α -amyrin
13.	apigenin
14.	astragaline
15.	Kaempferol
16.	quercetin

17.	vitexin
18.	9-acetamido-3,4dihydropyrido-(3,4-b) indole
19.	Amino-n-butyric acid
20.	Betaine
21.	β -carotene
22.	Daucosterol
23.	Deoxyvasicine
24.	Deoxyvasicinone
25.	Violanthin
26.	Vasnetine
27.	Desmethoxyaniflorine
28.	Rhamnoxylvitexin
29.	2"-O-xylosylvitexin
30.	Isovitexin
31.	3-hydroxyanisotone
32.	Epitaraxerol
33.	2',4-dihydroxychalcone4-O- β -D glucopyranoside
34.	5-hydroxy vasicine
35.	Luteolin
36.	umbeliferone
37.	3',4'-Dihydroxyflavonol
38.	Kaempferitrin
39.	10H-Quindoline
40.	Jusbetonin
41.	Allantoin
42.	Taiwanin E
43.	Taiwanin E methyl ether
44.	Justicidin E
45.	Isolariciresinol
46.	Justiciresinol
47.	Xanthoxylol
48.	Podophyllotoxin
49.	Heliobupthalmin
50.	Sesamin
51.	Chinensinaphthol methyl ether
52.	Justalakonin

53.	Cleistanthin B
54.	Patentiflorin A
55.	Patentiflorin B
56.	Tuberculatin
57.	Glyodin
58.	Vasakin
59.	Helioxanthin
60.	Justicidin B
61.	Diphyllin
62.	Justicidin A
63.	Justicidinose A
64.	Justicidinose C
65.	Justicidinose B
66.	Elenoside
67.	Diphyllin apioside
68.	Diphyllin apioside-5-acetate
69.	4'-Dimethyl chinensis naphthol methyl ether
70.	3-methylheptanone
71.	3-hydroxy-oleannane-5ene
72.	37-hydroxyhentetracontan-19-one
73.	37-hydroxyhexatetracont-1-en-15one
74.	Hydroxyl oxychalcone
75.	3 α -hydroxy-D-friedoolean-5-ene
76.	2'-glucosyl-4-hydroxyoxychalcone
77.	7-methoxy-vasicinone
78.	7-Methoxyvasicinone hydrate
79.	5-methoxyvasicinone
80.	Maiontone
81.	Vasinol
82.	Adhatodic acid
83.	vasicinine
84.	6-hydroxy Pegamine
85.	Adhavaasinone
86.	1,2,3,9-tetrahydro-5methoxy-pyrrolo[2,1b]quinazoline-3-ol
87.	vasicine acetate

Table S2: Phytocompounds with structure in PubChemdatabase

S.No.	Name of phytocompounds
1.	10h-quindoline
2.	2',4-dihydroxychalcone4-O- β -D glucopyranoside
3.	2-acetyl benzyl amine
4.	2"-O-xylosylvitexin
5.	3',4'-dihydroxyflavonol
6.	3-hydroxyanisotine
7.	5-hydroxy vasicine
8.	9-acetamido-3,4dihydropyrido-(3,4-b) indole
9.	Adhatodine
10.	Allantoin
11.	Amino-n-butyric acid
12.	Anisotine
13.	Apigenin
14.	Astragalin
15.	Betaine
16.	Chinensinaphthol methyl ether
17.	Cleistanthin B
18.	Daucosterol
19.	Deoxyvasicine
20.	Deoxyvasicinone
21.	Desmethoxyaniflorine
22.	Diphyllin apioside
23.	Diphyllin
24.	Diphyllin apioside-5-acetate
25.	Elenoside
26.	Epitaraxerol
27.	Glyodin
28.	Heliobupphthalmin
29.	Helioxanthin
30.	Isolariciresinol
31.	Isovitexin
32.	Jusbetonin
33.	Justalakonin

34.	Justicidin A
35.	Justicidin B
36.	Justicidin E
37.	Justicidinoside A
38.	Justicidinoside B
39.	Justicidinoside C
40.	Justiciresinol
41.	Kaempferitrin
42.	Kaempferol
43.	Luteolin
44.	Patentiflorin A
45.	Patentiflorin B
46.	Podophyllotoxin
47.	Quercetin
48.	Rhamnoxylvitexin
49.	Sesamin
50.	Taiwanin E
51.	Taiwanin E methyl ether
52.	Tritricontane
53.	Tuberculatin
54.	Umbeliferone
55.	Vasakin
56.	Vasicine
57.	Vasicinolone
58.	Vasicinone
59.	Vasicol
60.	Vasicoline
61.	Vasicolinone
62.	Vasnetine
63.	Violanthin
64.	Vitexin
65.	Xanthoxylol
66.	A-amyrin
67.	B-carotene
68.	B-sitosterol

Table S3: ADME/T properties of phytochemicals (Docking affinity less than or equal to -7 kcal/mol)

S. No.	Compound	Absorption		Distribution	Metabolism		Excretion	Toxicity	
		Water solubility	Intestinal absorption (human)	BBB Permeability	CYP 3A4 substrate	CYP 3A4 inhibitor	Total clearance	Max. Tolerated dose (human)	Oral acute toxicity
		Numerical (log mol/L)	Numerical (% Absorbed)	Numerical (log BB)	Categorical (Yes/No)	Categorical (Yes/No)	Numerical (log ml/min/kg)	Numerical (log mg/kg/day)	Numerical (mol/kg)
1.	10h-quinoline	-4.852	94.487	0.349	Yes	Yes	0.797	-0.124	2.298
2.	3',4'-dihydroxyflavonol	-1.137	94.875	-0.199	No	No	0.731	0.314	1.99
3.	3-hydroxyanisotone	-3.701	84.426	-0.257	Yes	Yes	0.678	-0.269	2.317
4.	9-acetamido-3,4-dihydropyridone-(3,4-b)	-3.125	94.655	0.127	No	No	0.413	-0.338	3.301

	indole								
5.	Adhatodine	- 1.27 8	75.4 88	- 0.17 4	No	No	0.579	0.037	2.10 1
6.	Anisotine	- 3.72 8	97.7 16	- 0.36 8	Yes	No	0.724	- 0.356	2.33 6
7.	Apigenin	- 3.38	91.5 66	- 0.90 3	No	No	0.595	0.337	1.97 8
8.	Chinensinap thol methyl ether	- 4.71 6	100	- 0.96 1	Yes	No	0.461	0.307	3.05 3
9.	Deoxyvasici ne	- 3.78 8	93.5 74	0.44 2	Yes	No	0.125	0.264	2.62 6
1 0.	Deoxyvasici none	- 1.72 2	99.0 37	- 0.07 9	No	No	0.749	- 0.166	2.07
1 1.	Diphyllin	- 4.68 1	96.5 04	- 0.85 8	Yes	Yes	0.305	0.137	2.52 4
1 2.	Heliobuphth almin	- 4.66 3	100	- 1.11 8	Yes	Yes	0.057	0.489	2.74 7
1 3.	Helioxanthi n	- 5.03 7	98.9 62	- 0.05 7	Yes	Yes	0.281	0.181	2.87 8
1	Isolariciresi	-	74.2	-	No	No	0.477	0.531	2.44

4.	nol	3.04	9	0.93 9					9
1 5.	Justicidin B	- 5.31 1	99.8 22	- 0.71 6	Yes	Yes	0.35	0.121	2.84 5
1 6.	Justicidin D	- 4.18 4	100	- 0.92 6	Yes	No	0.25	0.339	3.06 6
1 7.	Justicidin E	- 3.98 9	100	- 0.48 7	Yes	No	0.221	0.268	2.92 7
1 8.	Justicidin A	- 5.23	98.9 59	- 0.95 1	Yes	No	0.418	0.277	2.92 1
1 9.	Justiciresinol	- 4.61 8	71.7 91	- 1.03 8	Yes	Yes	0.176	0.276	2.10 9
2 0.	Kaempferol	- 3.28 2	80.0 64	- 1.06 5	No	No	0.496	0.774	2.19 7
2 1.	Luteolin	- 3.29 4	82.1 75	- 1.14 5	No	Yes	0.568	0.564	2.45 3
2 2.	Podophyllotoxin	- 3.97 1	100	- 0.82 1	Yes	Yes	0.205	-0.45	2.51 2
2 3.	Quercetin	- 2.92 5	77.2 07	- 1.09 8	No	No	0.407	0.499	2.47 1

24.	Sesamin	-4.173	98.218	-0.147	Yes	Yes	-0.096	0.372	2.767
25.	Taiwanin E	-4.007	97.826	-0.913	Yes	No	0.233	0.261	3.035
26.	Taiwanin E methyl ether	-4.027	100	-0.917	Yes	No	0.334	0.445	3.125
27.	Vasicilonone	-4.425	98.054	0.605	Yes	No	0.789	-0.113	2.239
28.	Vasicine	-2.052	75.497	-0.059	No	No	0.591	0.18	2.671
29.	Vasicinone	-1.278	75.488	-0.174	No	No	0.579	0.037	2.101
30.	Vasicoline	-4.815	92.372	0.596	Yes	No	0.609	0.127	2.592
31.	Vasicolinone	-4.425	98.054	0.605	Yes	No	0.789	-0.113	2.239
32.	Xanthoxylol	-3.688	94.756	-0.578	Yes	Yes	-0.046	-0.583	2.211

Table S4: Protein-ligand interaction profile of FDA approved drugs with SARS-CoV 2 Target protein

S · N o ·	Protein	P D B I D	Ligand	Binding affinity (kcal/ mol)	Amino acid residues involved and distance (Å)	
					Hydrogen bonding	Hydrophobic interactions
1	Spike protein	6 C R V	Daru navi r	- 1 0. 3	738A TYR (3.37), 977C ARG (3.28), 977C ARG (2.46), 980A THR (2.79), 980C THR (3.01), 980C THR (2.43), 980C THR (2.70), 984A GLN (2.78)	738C TYR (3.76), 741A PHE (3.23), 952C PHE (3.75), 973A VAL (3.64), 976A ASP (3.88), 977A ARG (3.67), 980B THR (3.34), 980C THR (3.6)
2	Envelope protein	5 X 2 9	Daru navi r	- 1 0. 6	-	23D PHE (3.7), 23D PHE (3.4), 26D PHE (3.82), 27D LEU (3.28), 29E VAL (3.46), 29E VAL (3.63), 30D THR (3.95), 31D LEU (3.57), 31E LEU (3.57), 46D ILE (3.99), 47D VAL (3.85), 57D TYR (3.79), 57D TYR (3.8), 57D TYR (3.68)
3	Membrane protein	3 I 6 G	Daru navi r	- 1 0. 2	26B TYR (2.50), 30A ASP (2.56), 57B SER (3.32), 58B LYS (2.89), 212A GLU (2.28), 212A GLU (2.36), 233A THR	6A ARG (3.87), 27A TYR (3.75), 27A TYR (3.84), 27A TYR (3.98), 58B LYS (3.71), 63B TYR (3.8), 63B TYR (3.62), 235A PRO (3.7), 235A PRO, 241A PHE (3.9), 241A PHE (3.73)

					(2.41), 233A THR (2.39)	
4	Main protease	6 L U 7	Saquinavir	- 8. 6	143A GLY (3.14), 144A SER (2.34), 145A CYS (2.59), 164A HIS (2.30), 166A GLU (2.36), 166A GLU (3.45)	41A HIS (3.48), 49A MET (3.81), 165A MET (3.33), 166A GLU (3.95), 167A LEU (3.92), 168A PRO (3.53), 187A ASP (3.58), 189A GLN (3.94), 189A GLN (3.25)
5	Spike protein receptor binding domain	6 M 0 J	Hydroxychloroquine	- 1 0. 1	208A GLU (3.41), 208A GLU (2.78)	95A LEU (3.93), 98A GLN (3.83), 209A VAL (3.82), 209A VAL (3.82), 210A ASN (3.68), 212A VAL (3.96), 565A PRO (3.75)
6	ORF 3a	6 X D C	Darunavir	- 9. 7	63A ILE (2.83), 75A LYS (2.23), 78A HIS (2.41), 78A HIS (2.59), 122B ARG (2.48), 126B ARG (2.27), 142B ASP (3.02), 206B TYR (2.76)	61A LYS (3.65), 122B ARG (3.97), 142A ASP (3.64), 206B TYR (3.66)
7	Non structural protein 3	6 W X D	Darunavir	- 8. 3	157A ASP (2.55)	23A ILE (3.19), 49A VAL (3.69), 52A ALA (3.49), 126A (LEU), 131A ILE (3.53), 132A PHE (3.69), 155A VAL (3.72), 156A PHE (3.43), 160A LEU (3.41), 160A LEU (3.76)
8	Non structural protein 9	2 G 9 T	Atv aquone	- 8. 8	41A VAL (2.48)	39A ARG (3.92), 40A PHE (3.52), 40A PHE (3.33), 41A VAL (3.7), 41A VAL (3.98), 56A PHE (3.95), 91A ILE (3.59)

9	Non structural protein 10	6 V W W	Saquinavir	- 1 0. 4	94E GLY (3.18), 96F TYR (3.27)	21L VAL (3.4), 23L PRO (3.84), 42E VAL (3.64), 57F VAL (3.69), 58F THR (3.95), 76L TYR (3.76), 76L TYR (3.73), 81L ILE (3.64), 84L PRO (3.56), 96E TYR (3.93), 96F TYR (3.66)
10	Non structural protein 15	6 V X S	Ivermectin	- 1 0. 6	46A ASN (3.32), 46B ASN (2.57), 52A VAL (2.19)	-